



## A metal-organic framework-based amperometric sensor for the sensitive determination of sulfite ions in the presence of ascorbic acid

Raissa Tagueu Massah<sup>a</sup>, Tobie J. Matemb Ma Ntep<sup>b,c</sup>, Evangeline Njanja<sup>a</sup>, Sherman Lesly Zambou Jiokeng<sup>a</sup>, Jun Liang<sup>c,d</sup>, Christoph Janiak<sup>c</sup>, Ignas Kenfack Tonle<sup>a</sup>

<sup>a</sup> Electrochemistry and Chemistry of Materials, Department of Chemistry, University of Dschang, P.O. Box 67, Dschang, Cameroon

<sup>b</sup> Department of Chemistry, Faculty of Science, University of Bamenda, P.O. Box 39, Bamili, Cameroon

<sup>c</sup> Institut für Anorganische Chemie und Strukturchemie, Heinrich-Heine-Universität Düsseldorf, Universitätsstraße 1, D-40225 Düsseldorf, Germany

<sup>d</sup> Hoffmann Institute of Advanced Materials, Shenzhen Polytechnic, 7098 Liuxian Blvd, Nanshan District, Shenzhen 518055, China

### ARTICLE INFO

#### Keywords:

Sulfite  
Ascorbic acid  
Carbon paste electrode  
Metal-organic frameworks  
Voltammetry  
Food quality control

### ABSTRACT

A carbon paste electrode modified with the MIL-101(Cr) metal-organic framework (MIL-101(Cr)-CPE) was prepared, characterized and assayed to the voltammetric detection of sulfite ions. Electrochemical impedance spectroscopy and cyclic voltammetry indicated a significant increase in charge transfer ability and real surface area ( $R_{ct} = 1.1 \text{ k}\Omega$  and  $S = 0.220 \text{ cm}^2$ ) of the MIL-101(Cr)-CPE in comparison with the bare CPE ( $R_{ct} = 7.8 \text{ k}\Omega$  and  $S = 0.031 \text{ cm}^2$ ). It was demonstrated by cyclic voltammetry that the oxidation of sulfite ions at the MIL-101(Cr)-CPE follows an irreversible and diffusion-controlled mechanism. Also, the peak current of sulfite ions was 1.5-fold more intense on MIL-101(Cr)-CPE compared to the unmodified CPE. An analytical method was further developed, based on square wave voltammetry: under optimized experimental conditions, the MIL-101(Cr)-CPE electrode displayed a linear relationship between the oxidation peak current and the concentration of sulfite in the concentration range of  $2 \mu\text{M}$ – $70 \mu\text{M}$ , with a detection limit of  $0.58 \mu\text{M}$  ( $S/N = 3$ ). The sensor was furthermore exploited for the simultaneous determination of sulfite and ascorbic acid, which gave well separated anodic peak at  $0.35 \text{ V}$  and  $0.90 \text{ V}$  (vs. Ag/AgCl, 3 M KCl), respectively. The proposed method was further used to determine both analytes in commercial wines, thus establishing its applicability as inexpensive analytical tool for quality control.

### 1. Introduction

Sulfites in the form of bisulfite or metabisulfite (as shown in Table S1) are important additives (denoted as E220-E228) in food industry. They are widely used as preservative or enhancer for manufactured food and beverages [1]. However, while sulfites are safe for most people, a small number (5–10%) of persons are sulfite-allergic and can develop related health problems including dermatological, pulmonary, gastrointestinal, and cardiovascular symptoms [2,3]. Whatever the case, sulfites are toxic at high doses and are therefore subject to regulations by many legislative agencies [4]. In 1994, an acceptable daily intake (ADI) of  $0.7 \text{ mg kg}^{-1}$  body weight/day for sulfur dioxide equivalent was set by the European Commission's Scientific Committee on Food (SCF) [5]. The Food and Drug Administration (FDA) also requires that all food-stuffs and beverages containing at least  $10 \text{ ppm}$  ( $10 \text{ mg kg}^{-1}$  or  $10 \text{ mL L}^{-1}$ ) sulfite should be labeled accordingly, with a maximum concentration of up to  $50 \text{ mg L}^{-1}$  in beer and  $350 \text{ mg L}^{-1}$  in wine [6].

The detection and analysis of sulfites is necessary in quality control of manufactured food and beverage products, as well as in

environmental monitoring. In particular, low-cost, highly sensitive/selective, easily applicable, fast and accurate analytical methods are required to comply with the various sulfite-related regulations. The Monier-Williams method is the most commonly used technique to determine sulfites in food [7]. However, due to the long analysis time associated with this method, many other techniques have been investigated including spectrophotometry, high-performance liquid chromatography, chemiluminescence, flow injection analysis and electrochemical analysis [8–11]. Electroanalysis, whereby the current generated by direct sulfite oxidation is measured at electrodes, provides low cost instrumentation and simplicity [12]. Especially, using a carbon paste electrode (CPE) is very advantageous on account of the low cost, a wide potential window and the very low background current compared to solid/metal electrodes. A most important feature of CPE based electroanalysis is the ease of incorporating an electrode-modifier to enhance the sensitivity and/or selectivity of the sensor [13,14].

Several materials have already been investigated to modify CPEs, including graphene [15], gold nanoparticles [16], zeolites [17]. Recently, a new class of porous materials, the so-called Metal-Organic

<https://doi.org/10.1016/j.microc.2021.106569>

Received 16 April 2021; Received in revised form 17 June 2021; Accepted 22 June 2021

Available online 30 June 2021

0026-265X/© 2021 Elsevier B.V. All rights reserved.

Frameworks (MOFs) are increasingly been used as effective electrode modifiers [18,19]. This is due to the synergistic zeolitic behavior and the electroactivity of the incorporated metal in MOFs [20]. MOFs are crystalline materials made of organic linkers coordinatively connecting metal-oxo clusters to yield a void-containing network [21]. A stable MOF-modified electrode requires the employment of hydrothermally and chemically robust MOF [18]. In this regard, MIL-101(Cr)-modified CPE (MIL stands for Materials for Institute Lavoisier) has been identified as an excellent candidate for the electroanalysis of ascorbic acid, dopamine and uric acid [22,23]. MIL-101(Cr) is a highly robust chromium-terephthalate-based MOF of empirical formula  $[\text{Cr}_3(\mu_3\text{-O})\text{X}(\text{H}_2\text{O})_2(\text{BDC})_3]$  (X = F or OH, depending on synthesis conditions; BDC = benzene-1,4-dicarboxylate). It is a mesoporous material, whose structure displays two types of inner cages with diameters of 2.9 nm and 3.4 nm. The smaller cage is accessible through pentagonal windows of about 1.2 nm diameter, while the larger cage is accessible through both pentagonal and hexagonal windows of about 1.5 nm diameter [24]. In addition to its high hydrothermal and chemical stability, other benefits of MIL-101(Cr) include its huge BET specific surface area (up to 4000  $\text{m}^2 \cdot \text{g}^{-1}$ ), the electroactivity of Cr and the presence upon activation of coordinatively unsaturated Cr centers (open metal sites, OMS) in its structure, which act as Lewis acid sites [25,26]. As electrode component, an OMS-containing and highly porous MOF like MIL-101(Cr) could catalyze the oxidation of sulfite, while improving the rate of electron transfer and thereby the usual poor sensitivity of the electrode [23]. Moreover, it could enable a selective or simultaneous detection of sulfites with usual interfering species (in real food and drink samples) such as ascorbic acid (AA) [27]. It is well-known that AA is frequently used as food additive alongside with sulfites, on account of its antioxidant and stabilizing ability. Yet, AA is oxidized within the same potential range as sulfite, thus requiring highly selective analytical methods. However, there has been so far, no report of electroanalysis of sulfites at a MOF-modified CPE. In addition, simultaneous electrochemical analysis of sulfites and AA is rather scarcely reported [28,29].

Herein, we present the electrochemical detection of sulfite ions at a MIL-101(Cr)-modified carbon paste electrode. After the synthesis and characterization of the MIL-101 MOF material, the MIL-101(Cr)-CPE electrode was prepared and analyzed by cyclic voltammetry (CV) and electrochemical impedance spectroscopy. It was further exploited by means of a carbon paste electrode for the detection of sulfite ions solely and then simultaneously with ascorbic acid, both in prepared solutions and in commercial wine samples.

## 2. Materials and methods

### 2.1. Reagents

All chemicals were obtained commercially and used without further purification. They include chromium (III) nitrate nanohydrate (Cr  $(\text{NO}_3)_3 \cdot 9\text{H}_2\text{O}$ , 99%, Acros Organics), terephthalic acid ( $\text{H}_2\text{BDC}$ , 98%, Sigma-Aldrich), ethanol (EtOH, 99.99%, Sigma-Aldrich), *N,N*-dimethylformamide (DMF, 99.99%, Fischer Chemicals),  $\text{HNO}_3$  (65 wt%, Fischer Chemicals), perfluorobenzoic acid ( $\text{C}_6\text{F}_5\text{COOH}$ , 99%, Prolabo), graphite powder (99.85%, Fisher), silicone oil (Sigma-Aldrich), sodium sulfite ( $\text{Na}_2\text{SO}_3$ , 99%, Prolabo), ascorbic acid ( $\text{C}_6\text{H}_8\text{O}_6$ , 99%, Sigma-Aldrich), citric acid ( $\text{C}_6\text{H}_8\text{O}_7$ , 99.5%, Baker), tartaric acid ( $\text{C}_4\text{H}_6\text{O}_6$ , 98%, Fischer Chemical), lactose ( $\text{C}_{12}\text{H}_{22}\text{O}_{11}$ , 99%, Sigma-Aldrich), calcium chloride ( $\text{CaCl}_2$ , 98%, Qualikens), magnesium chloride ( $\text{MgCl}_2$ , 98%, Kermel), glucose ( $\text{C}_6\text{H}_{12}\text{O}_6$ , 95%, Sigma-Aldrich), sodium nitrate ( $\text{NaNO}_3$ , 99.99%, Prolabo), aspartic acid ( $\text{C}_4\text{H}_7\text{NO}_4$ , 99%, Merck) and orange II ( $\text{C}_{16}\text{H}_{11}\text{N}_2\text{NaO}_4\text{S}$ , 98.5%, Prolabo). White wine samples were purchased at random from local outlets. The supporting electrolyte for voltammetry experiments was 0.1 M acetate buffer solution (ABS) obtained by mixing appropriate amounts of sodium acetate ( $\text{CH}_3\text{COONa}$ , 98.5%, Prolabo) and glacial acetic acid ( $\text{CH}_3\text{COOH}$ , 99.8%, Fischer), and adjusted to pH 5 by the addition of sodium hydroxide (NaOH,

99.8%, Fischer). Distilled water was used to prepare all solutions.

### 2.2. Synthesis of MIL-101(Cr)

MIL-101(Cr) was hydrothermally synthesized following a previously reported method to obtain a fluoride free material [30]. Briefly, 1.92 g of chromium nitrate nonahydrate (4.8 mmol) and 0.813 g of terephthalic acid (4.9 mmol) were stirred in 24 mL water for 1 h. Afterward, 0.475 g nitric acid (4.9 mmol) was added and stirring was continued for an additional 10 min. The mixture was then transferred into a Teflon-lined stainless-steel autoclave, sealed and heated at 200 °C in a preheated oven for 15 h. After cooling to room temperature, the solid product was separated from the mother liquor by centrifugation. The solid was re-dispersed twice in DMF (45 mL) and stirred for about 8 h each time to remove unreacted reagents, and then centrifuged. DMF was exchanged by stirring the solid twice in ethanol (45 mL) for about 24 h. After centrifugation, the solid was dried in air for about 24 h before heating at 150 °C under vacuum for 20 h to yield the activated MIL-101(Cr). The material was then characterized by powder X-ray diffraction while its specific surface area was determined by  $\text{N}_2$  sorption/desorption experiments (BET method).

### 2.3. Preparation of the MIL-101(Cr)-modified carbon paste electrode

To prepare the MIL-101(Cr)-modified carbon paste electrode (MIL-101(Cr)-CPE), 2 mg of MIL-101(Cr) were mixed with 33 mg of graphite powder, and then 15 mg of silicone oil were added as a non-conductive binder to obtain a uniform paste. The paste was introduced into a teflon hole. The smooth surface of MIL-101(Cr)-CPE was obtained by polishing the electrode with a flat paper sheet. For comparison, a non-modified CPE was prepared by mixing 15 mg of silicone oil with 35 mg of graphite powder.

### 2.4. Instrumentation

Electroanalytical experiments were carried out on a Palmsens<sup>3</sup> potentiostat controlled by a computer, equipped with PStrace (version 4.8) software for recording electrochemical experimental curves, and Origin 6.0 software for plotting the curves. A conventional three-electrode system was used consisting of Ag/AgCl (3 M KCl) as a reference electrode, a platinum wire and MIL-101(Cr)-CPE (or CPE) as counter and working electrodes, respectively. Electrochemical impedance spectroscopy (EIS) was conducted over the frequency range of 1 kHz to 100 kHz with a potential amplitude of 10 mV in 0.1 M KCl solution containing 1 mM  $[\text{Fe}(\text{CN})_6]^{3-/4-}$ . Measurements of pH were carried out with a Metrohm 780 pH meter equipped with a glass electrode. Powder X-ray diffraction (PXRD) pattern was recorded on a Bruker D2 Phaser diffractometer equipped with a flat silicon, low background sample holder using Cu  $K\alpha_1/\alpha_2$  radiation with  $\lambda = 1.5418 \text{ \AA}$  at 30 kV covering 2 theta angles 5–50° with a scan speed of  $1.5^\circ \cdot \text{min}^{-1}$  at room temperature. Fourier transform infrared (FT-IR) spectra was obtained on a Bruker FT-IR Tensor 37 spectrometer in the 4000–550  $\text{cm}^{-1}$  region. Scanning electron microscopy (SEM) image was obtained using a JEOL JSM-6510LV QSEM advanced electron microscope with a LaB6 cathode at 5–20 keV. The sample was coated with gold using a JEOL JFC 1200 fine-coater. Nitrogen sorption isotherms were recorded with a Micromeritics ASAP 2020 automatic gas sorption analyzer at 77 K. The BET (Brunauer-Emmett-Teller) specific surface area and pore volume were evaluated from the nitrogen physisorption isotherms. Before the measurement, the sample was degassed at 150 °C under vacuum for 20 h.

### 3. Results and discussion

#### 3.1. Physico-chemical characterizations of MIL-101(Cr)

The metal–organic framework MIL-101(Cr) to be used as electrode modifier was synthesized hydrothermally and obtained as a fluoride-free microcrystalline powder of formula  $[\text{Cr}_3(\mu_3\text{-O})(\text{OH})(\text{H}_2\text{O})_2(\text{BDC})_3]$ . Powder X-ray diffraction (PXRD) patterns of the simulated and synthesized MIL-101(Cr) materials are presented in Fig. 1a. The PXRD pattern of the obtained material matches positively with the simulated PXRD of MIL-101(Cr), with main Bragg reflections characterized by diffraction peaks appearing at  $2\theta = 5.53, 5.92, 8.38, 9.02, 10.35$  and  $16.58$  [29,31]. Fig. 1b shows a SEM picture of MIL-101(Cr). The obtained material reveals octahedral shaped crystallites with a particle size of about 0.2–0.5  $\mu\text{m}$ . Particles with octahedral shape are a characteristic feature of MIL-101(Cr). The shape and the size are similar to data from a previous work [32]. The nitrogen sorption experiment at 77 K conducted with an activated sample of the obtained material (Fig. 1c) displays the characteristic type 1 isotherm (according to the IUPAC classification) of MIL-101(Cr) with secondary uptakes at  $P/P_0 \sim 0.1$  and  $P/P_0 \sim 0.2$ , corresponding to the presence of two kinds of microporous windows. The BET surface area and the total pore volume were calculated from the adsorption isotherm to be about  $3100 \text{ m}^2 \text{ g}^{-1}$  and  $1.5 \text{ cm}^3 \text{ g}^{-1}$ , respectively. The FTIR spectrum of MIL-101(Cr) in the  $1800 - 500 \text{ cm}^{-1}$  region is depicted in Fig. 1d. It is characterized by O–C–O symmetrical stretching vibration at  $1625$  and  $1400 \text{ cm}^{-1}$ , C = C stretching vibration at  $1510 \text{ cm}^{-1}$  and C–H deformation vibration appearing at  $1160, 1018, 884$  and  $744 \text{ cm}^{-1}$  [33,34] that together confirm the presence of the dicarboxylate moieties in MIL-101(Cr).

#### 3.2. Electrochemical characterization of MIL-101(Cr)-CPE

In order to evaluate the electroactive surface of MIL-101(Cr) material and its ability to bind ionic species, cyclic voltammetry (CV) was performed using  $[\text{Fe}(\text{CN})_6]^{3-}$  and  $[\text{Ru}(\text{NH}_3)_6]^{3+}$  as redox probes. The CV curves shown in Fig. 2a, reveal a progressive accumulation of  $[\text{Fe}(\text{CN})_6]^{3-}$  ions within the material by continuous cyclic scanning, yielding peak currents larger than that measured from the simple carbon paste electrode. This observation can be explained by favorable interactions between  $[\text{Fe}(\text{CN})_6]^{3-}$  anions and the Cr cations of the MIL-101(Cr) MOF material. This result shows that this material bears positive surface charges since it accumulates  $[\text{Fe}(\text{CN})_6]^{3-}$  ions. This electrode can therefore be used for the electroanalysis of negative ions such as sulfite ions in solution. A proof of this was brought by analyzing by the same electrode  $[\text{Ru}(\text{NH}_3)_6]^{3+}$  positively charged ions. One can notice on Fig. 2b recorded in similar conditions that there is just a detection of  $[\text{Ru}(\text{NH}_3)_6]^{3+}$  ions but not an accumulation of these ions, since the current peak remains constant for successive cyclic scans. The observed signal is attributed to the adsorption of the redox probe by the porous MOF material at the electrode. Furthermore, electrochemical impedance spectroscopy (EIS) was used to assess the electron transfer rate of CPE and MIL-101(Cr)-CPE using the  $[\text{Fe}(\text{CN})_6]^{3-/4-}$  redox couple. The obtained Nyquist diagrams on Fig. 2c demonstrated that the bare CPE (curve 1) has a more pronounced semi-circle than MIL-101(Cr)-CPE (curve 2) corresponding to a process limited by electron transfer. The CPE has therefore a quite larger electron-transfer resistance ( $R_{ct}$ ) value of about  $7.8 \text{ k}\Omega$  compared to that of MIL-101(Cr)-CPE, whose value is  $1.1 \text{ k}\Omega$ . The modification of CPE with MIL-101(Cr) results in a high electron transfer ability of the composite. These results suggest that MIL-101(Cr) can be prominently exploited for electrochemical applications.

To gain more information on the reactivity of both CPE and MIL-101

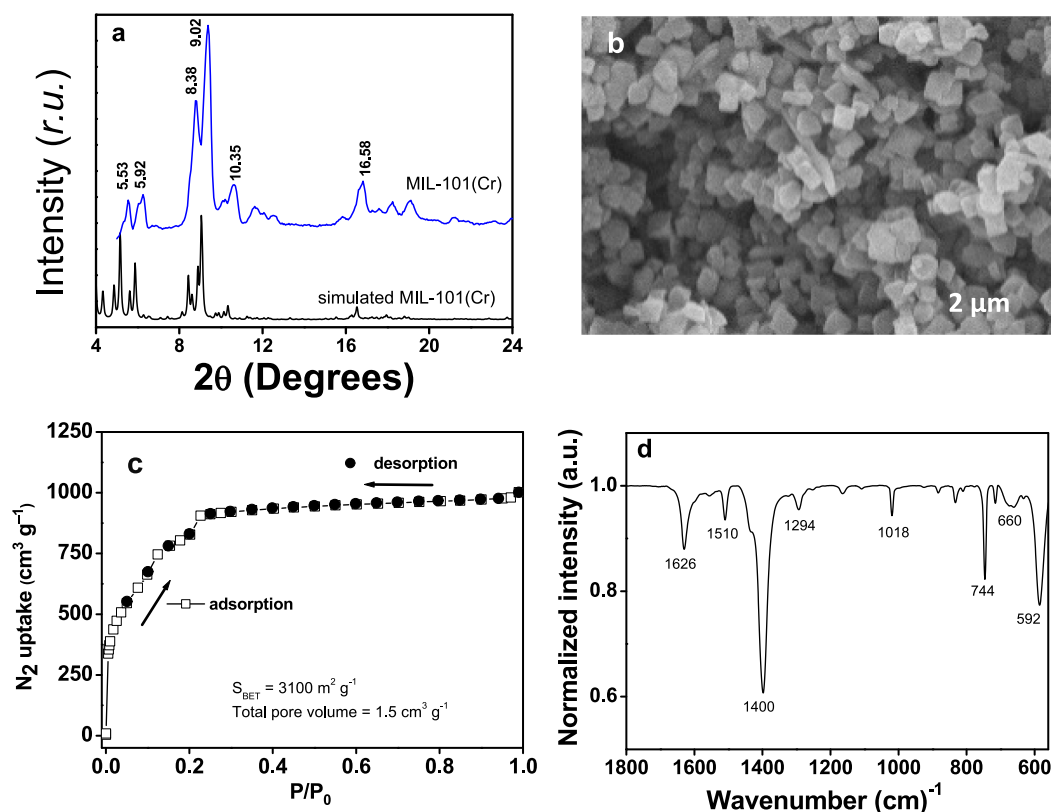
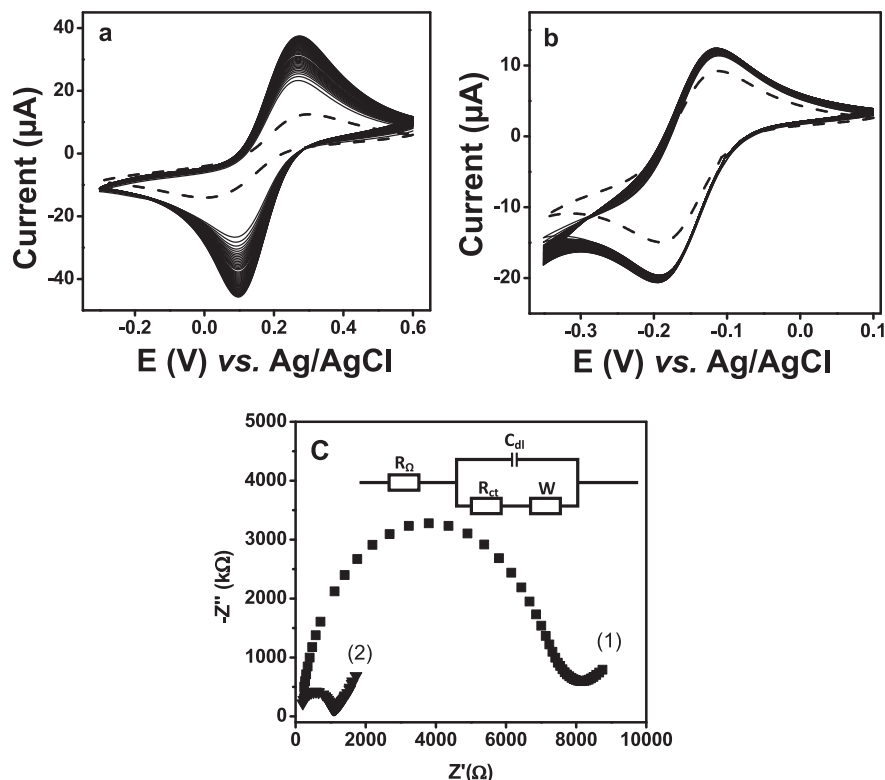


Fig. 1. (a) Powdered XRD patterns of simulated MIL-101(Cr) and MIL-101(Cr), (b) SEM image of MIL-101(Cr), (c)  $\text{N}_2$  adsorption–desorption isotherms on the MIL-101(Cr) and (d) FTIR spectra of MIL-101(Cr).



**Fig. 2.** Multisweep cyclic voltammograms recorded at  $50 \text{ mV s}^{-1}$  in  $0.1 \text{ M KCl}$  solution containing: (a)  $1 \text{ mM } [\text{Fe}(\text{CN})_6]^{3-}$  and (b)  $1 \text{ mM } [\text{Ru}(\text{NH}_3)_6]^{3+}$  using MIL-101 (Cr)-CPE. The dot line in (a) and (b) corresponds to bare CPE, and (c) Nyquist diagrams recorded in  $0.1 \text{ M KCl}$  containing  $1 \text{ mM } [\text{Fe}(\text{CN})_6]^{3-/4-}$  on CPE (1) and MIL-101(Cr)-CPE (2).

(Cr)-CPE, their electroactive surface areas were calculated by varying the potential scan rate on these electrodes during CV experiments, performed in  $0.10 \text{ M KCl}$  solution containing  $10^{-3} \text{ M } [\text{Fe}(\text{CN})_6]^{3-}$ . Fig. SI (1) (Supporting electronic data) shows the results obtained for scan rates between  $10$  and  $120 \text{ mV s}^{-1}$ . The anodic current responses increase linearly with the square root of scan rate ( $v^{1/2}$ ) according to the following expressions:  $I_{pa} = 2.32 \times 10^{-5} v^{1/2} + 1.36 \times 10^{-6}$  ( $R^2 = 0.995$ ) and  $I_{pa} = 1.63 \times 10^{-4} v^{1/2} + 4.64 \times 10^{-6}$  ( $R^2 = 0.996$ ), for CPE and MIL-101(Cr)-CPE respectively. The recorded currents follow the Randles-Sevcik equation  $I = (2.69 \times 10^5) n^{3/2} A C D^{1/2} v^{1/2}$  (where  $I$  is the peak current,  $n$  the number of electrons transferred,  $A$  the electroactive area ( $\text{cm}^2$ ),  $D$  the diffusion coefficient of  $[\text{Fe}(\text{CN})_6]^{3-}$  in a  $0.1 \text{ M KCl}$  solution,  $C$  the concentration of  $[\text{Fe}(\text{CN})_6]^{3-}$  ( $\text{mol cm}^{-3}$ ) and  $v$  the potential scan rate ( $\text{V s}^{-1}$ )). By exploiting the Randles-Sevcik equation, the slopes of the  $I$  vs.  $v^{1/2}$  plots and  $D$  value for  $[\text{Fe}(\text{CN})_6]^{3-}$  ( $7.6 \times 10^{-6} \text{ cm}^2 \text{ s}^{-1}$ ) [22], electroactive surface areas of  $0.031 \text{ cm}^2$  and  $0.220 \text{ cm}^2$  were calculated for CPE and MIL-101(Cr)-CPE, respectively. This indicates that the MIL-101(Cr) induces a 7-fold higher electroactive surface area of the modified electrode.

### 3.3. Electrochemical behavior of sulfite ions on MIL-101(Cr)-CPE

Before applying the MIL-101(Cr)-CPE for the electroanalysis of sulfite ions, the electrochemical behavior of these ions was studied by CV. Fig. 3 presents the voltammograms recorded in  $0.1 \text{ mM ABS}$  (pH 5.2) containing  $0.7 \text{ mM}$  sulfite ions, when the working electrode was either the unmodified CPE (curve b) and MIL-101(Cr)-CPE (curve c). As noticed, sulfite ions were oxidized at  $1.13 \text{ V}$ , leading to peak current values of  $26.25 \mu\text{A}$  and  $17.63 \mu\text{A}$  at MIL-101(Cr)-CPE and CPE respectively. The increase observed in anodic peak current is an indication that MIL-101(Cr) enhances the oxidation of sulfite ions. The good performance of the MIL-101(Cr)-modified CPE is also due to its porosity and

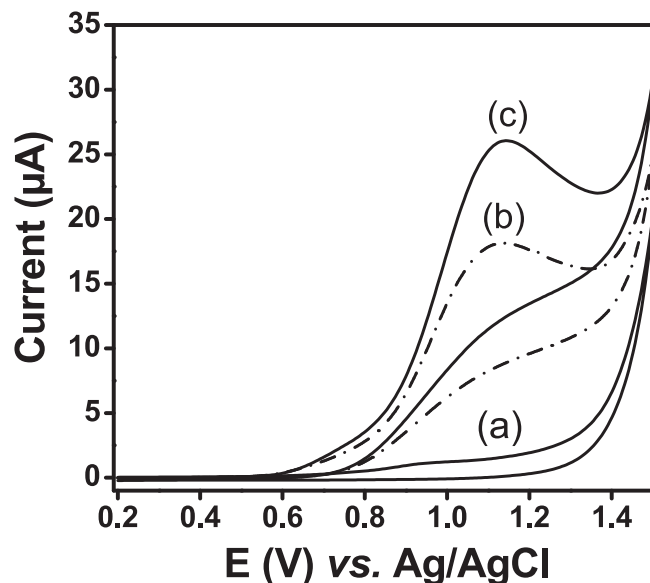


**Fig. 3.** Cyclic voltammograms of  $0.7 \text{ mM}$  sulfite ions solution recorded in  $0.1 \text{ M ABS}$  (pH 5.2), (a) blank solution, (b) on CPE and (c) on MIL-101(Cr)-CPE ( $v = 50 \text{ mV s}^{-1}$ ).

large surface area which can offer more adsorption sites and improve the electrochemical response.

### 3.4. Effect of potential scan rate

To determine key electrochemical kinetic parameters related to the

electron transfer process at the MIL-101(Cr)-CPE, the effect of potential scan rate ( $\nu$ ) was studied. Fig. 4a presents the current response ( $I_p$ ) obtained by varying  $\nu$  between 10 and 100  $\text{mV}\cdot\text{s}^{-1}$  when the CPE modified by the MOF was dipped in 0.1 M ABS (pH 5.2) containing 0.7 mM sulfite ions. As observed in the previous section, an irreversible peak of sulfite ions was obtained on each voltammogram for investigated scan rates. Upon this variation, the anodic peak currents gradually increased with the potential scan rate. At the same time, these peak currents show linear dependence with the square root of the potential scan rate ( $\nu^{1/2}$ ): ( $I_{pa} = 0.406 + 3.722 \nu^{1/2}$ ,  $R^2 = 0.998$ ) (Fig. 4b). This indicates a diffusion-controlled process, a fact that was also confirmed by plotting the double logarithmic of  $I_{pa}$  vs scan rate (Fig. SI (2a)) characterized by a slope equal to 0.48 (close to the theoretical 0.5 value for diffusion-controlled electron-transfer mechanism) [35]. With the increase of scan rate, the oxidation peak potentials ( $E_{pa}$ ) shifted to the positive direction. The relationship between the peak potential ( $E_p$ ) and  $\log \nu$  (Fig. SI (2b)):  $E_p = 0.0012 + 6.405 \times 10^{-5} \log \nu$  ( $R^2 = 0.959$ ), confronted with the Laviron's equation for an irreversible electrode process:  $E_p = E^\circ + \frac{(2.303 \times RT)}{\alpha n F} \log \left( \frac{RTk_f^\circ}{\alpha n F} \right) + \frac{(2.303 \times RT)}{\alpha n F} \log \nu$  [36] allowed to obtain some kinetic parameters. By assuming the value of  $\alpha$  to be equal to 0.5

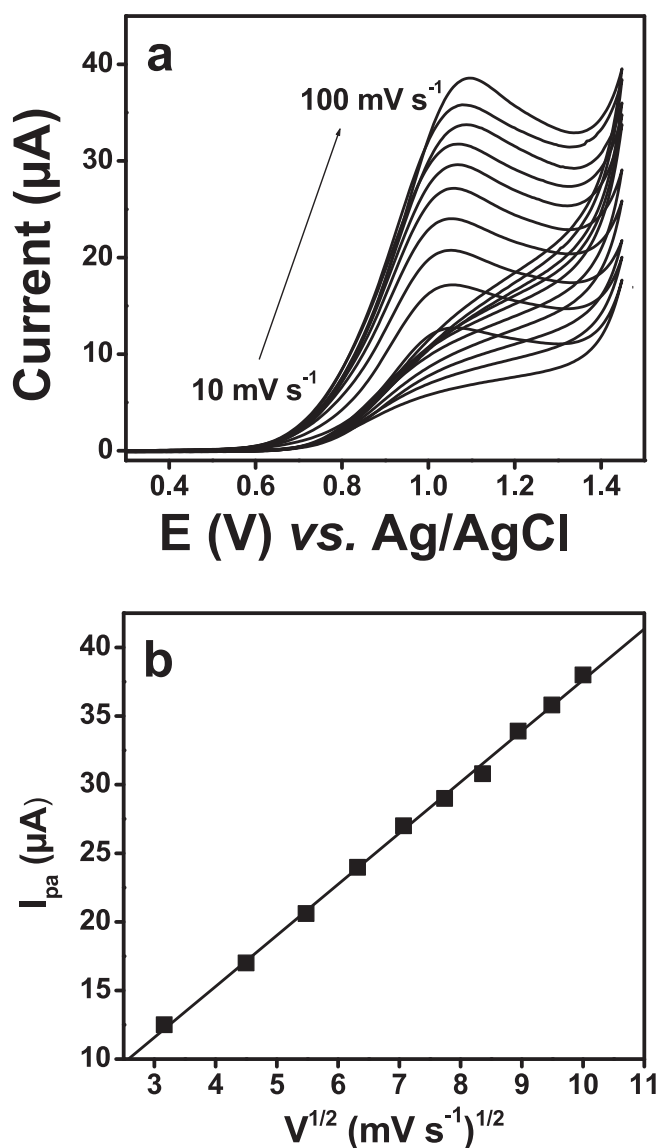


Fig. 4. (a) Cyclic voltammograms recorded in 0.1 M ABS (pH 5.2) containing 0.7 mM sulfite ions on MIL-101(Cr)-CPE at different scan rates (10 to 100  $\text{mV}\cdot\text{s}^{-1}$ ) and (b) peak current as a function of  $\nu^{1/2}$ .

[28], the number of electron transferred ( $n$ ) in the electrooxidation of sulfite ions was calculated to be  $1.87 \approx 2$ .

### 3.5. Effect of the amount of MIL-101(Cr) in the carbon paste working electrode

In order to determine the optimum amount of MIL-101(Cr) generating the best electrode response, CPEs containing respectively 0, 2, 4, 6, 8 and 10 %wt of MIL-101(Cr) were prepared and tested for the determination of sulfite ions. The various mixtures were made of  $x$  mg of MIL-101(Cr), (35- $x$ ) mg of graphite powder and 15 mg of silicone oil ( $x = 0, 1, 2, 3, 4$  and 5). The peak currents of sulfite ions increased with increasing amount of MIL-101(Cr) for  $x$  values from 0 to 2 and then decreased to 5, as shown in Fig. SI (3). This tendency could be attributed to the high porosity and OMS of MIL-101(Cr) that contribute to increase the conductivity of the MIL-CPE electrode till a maximum MIL-101(Cr) of 10 %wt. Above this value, the insulating nature of the MOF starts to dominate, thereby limiting the activity of the electrode. The modified electrode containing 2 mg of MIL-101(Cr) was therefore used for subsequent investigations.

### 3.6. Effect of pH on the peak current and potential

The effect of pH of the detection medium was studied by measuring both the oxidation peak current and potential of sulfite at pH values varying between 3.5 and 6.5 (Fig. 5). It was observed that the oxidation peak potential of sulfite ions linearly decreased with an increase in pH (Fig. 5a) according to the following equation:  $E_p = 1.454 - 0.073 \times \text{pH}$  ( $R^2 = 0.997$ ). As previously obtained by Asafneh et al. (2008) [37], this result indicates that protons are involved in the reaction process at the electrode surface. The value of the slope ( $-0.073 \text{ V/pH}$ ) close to the theoretical Nernstian value ( $-0.059 \text{ V/pH}$ ) suggested that an equal number of electrons and protons are involved in the oxidation of sulfite ions, thus corroborating the oxidation reactions given above. A 0.1 M ABS solution set at pH 5 was the optimum pH value, used in further experiments. Under the pH condition studied in Fig. 5,  $\text{HSO}_3^-$  is expected to be the most dominant electro-active reagent. Interestingly, the peak current is almost constant within the pH range of 3.5 to 5, with a current value of about 45  $\mu\text{A}$  after which the current drops abruptly to keep a fairly constant value of about 23  $\mu\text{A}$  in the 5.5–6.5 pH range (Fig. 5b). It was previously established that sulfite ions in solution are in equilibrium in the form of  $\text{HSO}_3^-$ ,  $\text{SO}_3^{2-}$  or  $\text{SO}_2$  depending on the pH value [38] according to the following scheme:  $\text{SO}_2 + \text{H}_2\text{O} \rightleftharpoons \text{HSO}_3^- + \text{H}^+ \rightleftharpoons \text{SO}_3^{2-} + 2\text{H}^+$ .

In the pH range 3.5–5,  $\text{HSO}_3^-$  species is predominant and is therefore oxidized following the reaction:  $\text{HSO}_3^- + \text{H}_2\text{O} \rightleftharpoons \text{HSO}_4^- + 2\text{H}^+ + 2\text{e}^-$ . For pH values between 5.5 and 6.5,  $\text{HSO}_3^-$  species is also present, but its concentration decrease with the increase in  $\text{SO}_3^{2-}$  ions. The best peak currents between pH 3.5 and 5, with a maximum current at pH 5 can be due either to the complexation of  $\text{HSO}_3^-$  ions with Cr cations or to the porosity of the material. On the other hand, the decrease observed after pH 5 could be due to the electrostatic repulsion between the  $\text{HSO}_3^-$  and  $\text{SO}_3^{2-}$  ions present in solution and electron pairs of oxygen in the hydroxy of terephthalic acid.

### 3.7. Calibration curve

Square wave voltammetry (SWV) is a powerful electroanalytical technique assuring great resolution of peaks, which is usually used for the determination at trace level of various inorganic and organic compounds. It was chosen to investigate the relationship between the peak current and the concentration of sulfite ions at MIL-101(Cr)-CPE. Fig. 6 shows the corresponding current responses obtained. The resulting calibration plot was linear over the concentration range of 2.0  $\mu\text{M}$  to 70.0  $\mu\text{M}$  sulfite (Inset of Fig. 6), following the equation  $I_{pa}(\mu\text{A}) = 0.227 + 0.095 \times C(\mu\text{M})$  where  $C$  is sulfite concentration. The sensitivity is  $0.095 \mu\text{A}\cdot\mu\text{M}^{-1}$  and the regression coefficient  $R$  is 0.999. Based on the

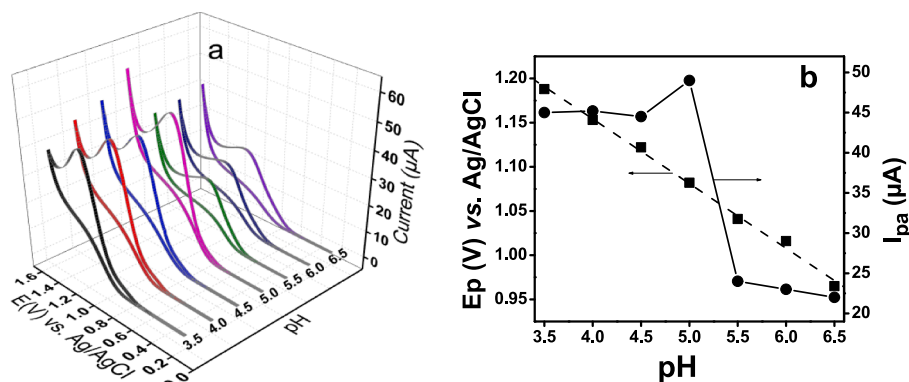


Fig. 5. (a) Effect of the pH of the detection medium on the electrochemical response of 0.7 mM of sulfite ions<sup>-</sup> in ABS on MIL-101(Cr)-CPE and (b) plot of  $I_{pa}$  versus pH and peak potential ( $E_p$ ) versus pH.

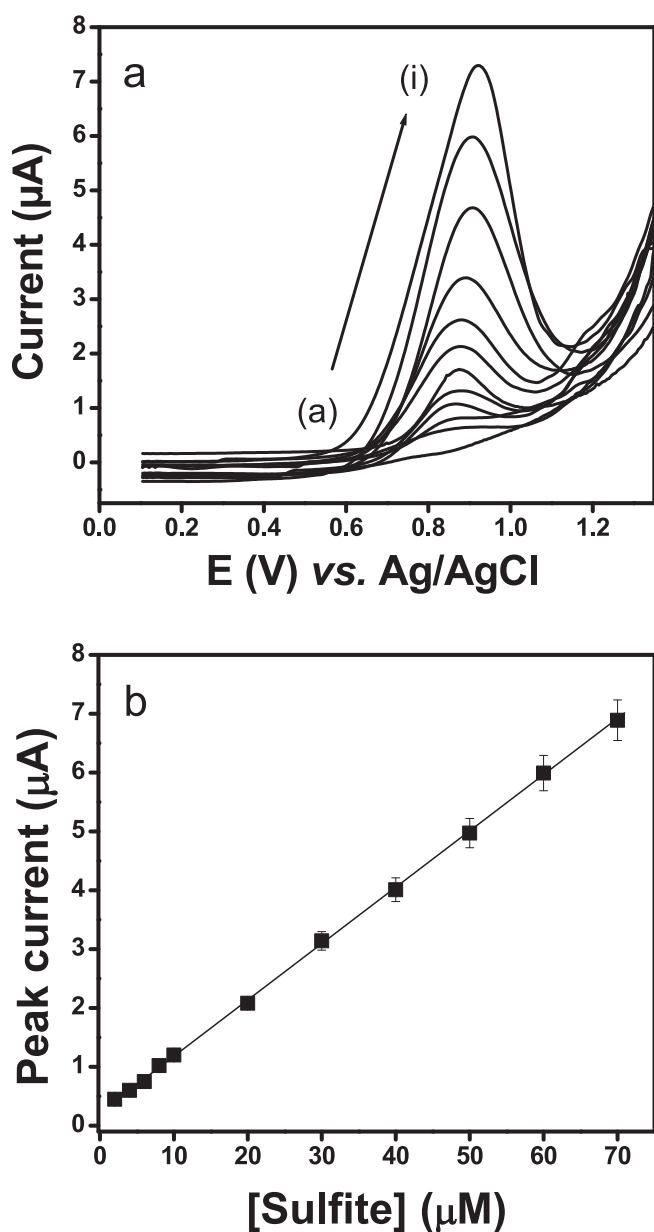


Fig. 6. (a) SWV responses for different concentrations of sulfite ions (a to i: 2, 4, 6, 8, 10, 20, 30, 40, 50, 60, 70 and 80  $\mu\text{M}$ ) in 0.1 M ABS (pH 5) at MIL-101(Cr)-CPE; and (b) Corresponding calibration graph.

signal-to-noise ratio 3, the limit of detection (LOD) was calculated using the equation  $\text{LOD} = 3S/m$  [39] where  $S$  is the standard deviation of blank and  $m$  is the slope of the regression line. The obtained value of LOD was 0.58  $\mu\text{M}$ , which was compared to some data reported for sulfite detection using other modified electrodes (Table 1). By analyzing these data, it appeared that the voltammetric determination of sulfite based on the MIL-101(Cr)-modified CPE electrode is a sensitive method. The repeatability of the proposed method was evaluated by performing five successive SWV experiments for analyzing a 0.05 M sulfite solution (in 0.1 M ABS at pH 5.0) under established optimized conditions, as shown in Fig. SI (4): a relative standard deviation (RSD) value of 3.5% was obtained, proving that the reproducibility was at an acceptable level. Additionally, the long-term stability of the MIL-101(Cr)-CPE was examined by recording the amperometric signal of 0.05 M sulfite solution once a day and for one week, the sensor being kept in 0.1 M ABS (pH 5) between measurements. The sensor displayed about 95% of its original response, a proof that it was quite stable.

### 3.8. Simultaneous determination of sulfite ions and ascorbic acid

Ascorbic acid is amongst the compounds that usually interfere in the determination of sulfite ions in food. It was necessary to explore the possibility of analyzing both compounds by using the MIL-101(Cr)-modified CPE sensor. Fig. 7 shows the voltammograms obtained in

Table 1

Comparison of the efficiency of some methods and electrodes in the determination of sulfite ions.

Working electrodes	Method	Detection medium (pH)	<sup>1</sup> LOD ( $\mu\text{mol L}^{-1}$ )	Reference
<sup>2</sup> CILE	SWV	<sup>3</sup> PBS (7.0)	4	[37]
Poly[Cu (salen)] Films/Pt	Chronoamperometry	KCl (6.0)	1.2	[40]
<sup>4</sup> MWCNT-CPE	SWV	<sup>5</sup> BRS (1.0)	16	[41]
<sup>6</sup> CBE	SWV	PBS (7.4)	6	[42]
<sup>7</sup> Ni/poly(4-AB)/SDS/CPE	Amperometry	PBS (11.0)	63	[43]
<sup>8</sup> Cyt c/SDH/MU-Au	Amperometry	Tris acetate (8.0)	0.044	[44]
MIL-101(Cr)-CPE	SWV	ABS (5.0)	0.98	This work

<sup>1</sup> LOD: Low limit of detection, <sup>2</sup>CILE: Carbon liquid ionic electrode, <sup>3</sup>PBS: Phosphate buffer solution, <sup>4</sup>MWCNT: Multiwalled carbon nanotubes, <sup>5</sup>BRS: Britton Robison solution, <sup>6</sup>CBE: Carbon black electrode, <sup>7</sup>Ni/poly(4-AB)/SDS: Ni/poly(4-aminobenzoic acid)/sodium dodecylsulfate/ Sodium Dodecyl Sulfate, <sup>8</sup>Cyt c: cytochrome c, SDH: Starkeya novella sulfite dehydrogenase, MU: 11-mercaptoundecanol.

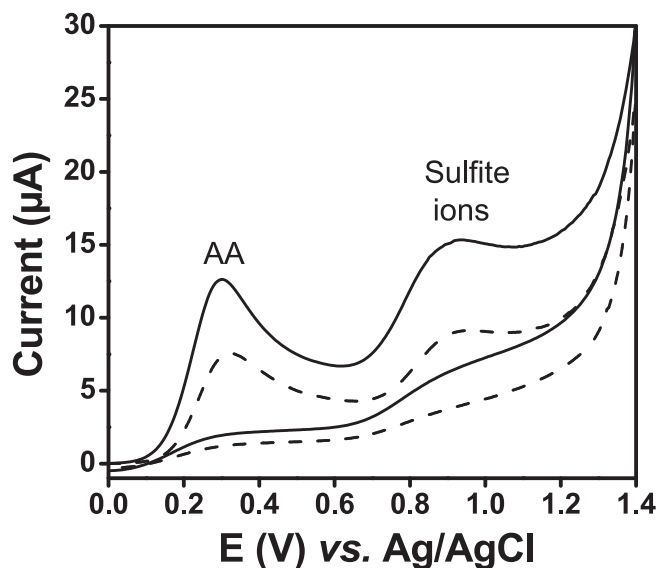


Fig. 7. Cyclic voltammograms of 0.4 mM AA and 0.4 mM sulfite recorded in 0.1 M ABS (pH 5.2) on CPE (black curve) and on MIL-101(Cr)-CPE (Dot line),  $v = 50 \text{ mV s}^{-1}$ .

cyclic voltammetry in a solution of acetate buffer pH 5 containing AA and sulfite in the same proportions (0.4 mM). In the presence of these compounds, two oxidation peak potentials were observed around 0.35 V and 0.9 V corresponding respectively to ascorbic acid and sulfite ions. The result obtained for the AA is in agreement with a previous one by Tshakourian et al. (2019) [23] regarding to the sensitivity of MIL-101(Cr)-CPE. It is also important to note that the current intensity obtained with MIL-101(Cr)-CPE for both compounds is about 1.5-fold that obtained with the bare CPE. In agreement with data previously reported in the literature, the oxidation of AA involved two electrons and two protons in acetate buffer solution according to the oxidation mechanism [28]:  $\text{C}_6\text{H}_8\text{O}_6$  (ascorbic acid)  $\rightarrow$   $\text{C}_6\text{H}_6\text{O}_6$  (dehydroascorbic acid) +  $2\text{e}^- + 2\text{H}^+$ . The peak separation of about 0.6 V then allowed the simultaneous determination of both compounds by SWV. Fig. 8 shows that the oxidation peak current increased linearly with increasing concentration of AA and sulfite within same linear concentration ranges. The linear regression equation of AA and sulfite were found to be  $I_{\text{pa}} (\mu\text{A}) = 0.067 + 0.0806 [\text{AA}] (\mu\text{M})$  ( $R^2 = 0.997$ ) and  $I_{\text{p}} (\mu\text{A}) = 0.258 + 0.0856 [\text{sulfite}] (\mu\text{M})$  ( $R^2 = 0.997$ ). The LODs was found to be 1.86  $\mu\text{M}$  and 1.90  $\mu\text{M}$  respectively for AA and sulfite.

### 3.9. Interference study and analytical application

The selectivity of MIL-101(Cr)-CPE towards sulfite ions and ascorbic acid was evaluated in the presence of other selected compounds including citric acid, lactose, orange II, glucose, aspartic acid, nitrate, magnesium and calcium ions at known concentrations (10, 40, 200 and 400  $\mu\text{M}$ ). The oxidation peak current response of solutions containing 40  $\mu\text{M}$  sulfite ions and AA with additional aforementioned species was measured at the MIL-101(Cr)-CPE in 0.1 M ABS pH 5. The recoveries of analyte signal relative to that of solution without interfering species are presented in Table 2. In some cases, the results obtained showed that the intensities of the oxidation peaks of sulfite ions and ascorbic acid were strongly affected, with recovery rates lower than 100%. Indeed, the highly porous MIL-101(Cr) MOF possesses a chromium atom and oxygen electron pairs in the hydroxy groups of terephthalic acid that are sensitive to most investigated compounds and ions. This fact leads to a competition for binding sites, which result in a decrease in the signal of sulfite ions and ascorbic acid. As main observation, it was noticed that citric acid and lactose interfere slightly on AA and sulfite signals when introduced at 0.25-fold concentration, and that aspartic acid does not

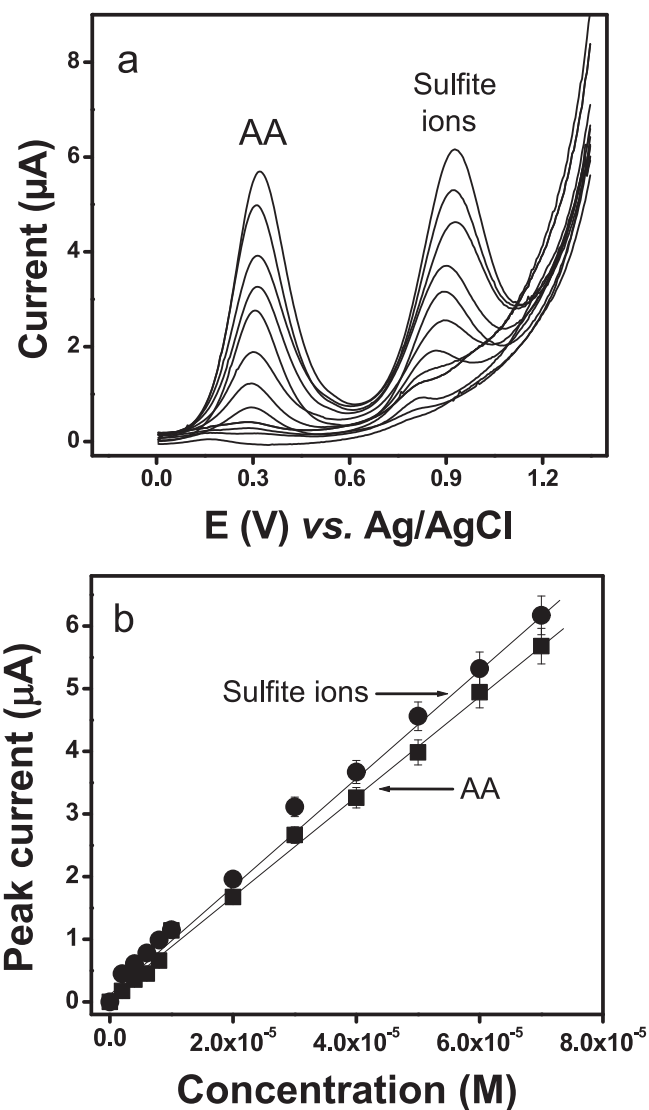


Fig. 8. (a) SWVs of MIL-101(Cr)-CPE in 0.1 M ABS (pH 5.0) containing different concentrations of sulfite and ascorbic acid (AA); (b) Plots of  $I_{\text{p}}$  vs. [AA] and  $I_{\text{p}}$  vs. [Sulfite].

interfere. However, glucose, orange II,  $\text{Mg}^{2+}$ ,  $\text{NO}_3^-$  and  $\text{Ca}^{2+}$  ions were the main interfering ions since they significantly influenced (more than 20% reduction) the responses of both the sulfite and AA analytes. When all species were added at equal concentration or in concentration above that of AA and sulfite ions, the peak currents of these analytes were more affected, a fact that somewhat limits the selectivity of the proposed sensor and suggest that it could be preferably used for media containing mostly sulfite and ascorbic acid and not the studied interferents.

The newly obtained MIL-101(Cr)-CPE sensor was finally used to determine the sulfite in presence of ascorbic acid contents in two commercial white wine samples (Cabernet-Sauvignon grape variety, from Spain and produced in 2019). The selected wine samples were analyzed without any purification or pretreatment. For comparison purposes and to control the accuracy of the developed electroanalytical method, the sulfite content of these samples was also determined by iodometry: A precise sample volume (1.00 mL) was added to 10 mL of ABS and a 2 mM iodine solution was added until equivalence. Starch was used as colored indicator. These determinations were carried out as quickly as possible, the end point being indicated by the formation of the colour blue. From the obtained results (Table 3), one can notice that the data of both iodometric and voltammetric determinations are in the same order of

**Table 2**Analyte signal recovery (%) at MIL-101(Cr)-CPE for the analysis of 40  $\mu\text{M}$  sulfite ions and AA in the presence of some potential interfering species.

Added species	Concentration of added ions (in $\mu\text{M}$ ) in relation to AA and sulfite ions concentrations							
	0.25-fold		1-fold		5-fold		10-fold	
	AA	sulfite	AA	sulfite	AA	sulfite	AA	sulfite
Citric acid	90.3	92.7	89.1	82.78	85.4	83.9	80.2	78.8
Aspartic acid	96.6	108.5	82.4	80.7	91.5	91.1	88.7	90.4
Orange II	79.3	41.7	83.7	55.9	81.5	80.7	72.8	93.4
Glucose	83.3	77.01	69.04	59.6	59.3	38.6	56.04	41.1
Lactose	95.8	58.2	104.6	58.1	97.6	50.8	94.5	40.9
Mg <sup>2+</sup>	53.3	60.0	52.9	55.9	53.7	59.5	48.4	55.4
Ca <sup>2+</sup>	79.9	89.6	72.9	86.5	76.4	87.7	79.9	86.2
NO <sub>3</sub> <sup>-</sup>	85.5	97.9	77.2	93.5	75.8	86.3	75.5	79.3

**Table 3**

Compared results from the determination of sulfite in 2 commercial white wine samples.

Sample	*Voltammetric method	*Iodometric method
	Sulfite (mg L <sup>-1</sup> )	Sulfite (mg L <sup>-1</sup> )
White Wine 1	85.95 $\pm$ 12.00	86.40 $\pm$ 9.00
White Wine 2	104.14 $\pm$ 13.00	108.10 $\pm$ 9.00

\*All values represent the mean value of three replicates.

magnitude as the difference between the mean values is not significant. Thus, the sulfite contents (85.95 mg L<sup>-1</sup> for wine sample 1 and 104.14 mg L<sup>-1</sup> for wine sample 2) in the studied samples could be considered to be correct. The voltammetric method proposed herein can be considered reliable, and can be used to determine sulfite in presence of AA in manufactured foodstuffs and beverages.

#### 4. Conclusion

A sensor based on a carbon paste electrode with the MOF MIL-101 (Cr) has been elaborated and optimized, then applied in the voltammetric determination of sulfite ions. Compared to the unmodified CPE, a seven-fold decrease of the charge resistance and seven-fold increase of the electroactive area were realized, due to the huge surface area and porosity of MIL-101(Cr), as well as the presence of unsaturated metal sites within its network. The new MIL-101(Cr)-CPE was highly sensitive to detect sulfite and simultaneously determine sulfite and ascorbic acid with well resolved peak potentials separation in real samples. The MIL-101(Cr) modified carbon paste electrode therefore is established as a highly efficient and inexpensive sensor for the detection of sulfite or simultaneous sulfite and ascorbic acid. This could be exploited by laboratories and personal in charge of quality control of manufactured food and beverages.

#### CRediT authorship contribution statement

**Raissa Tagueu Massah:** Writing - original draft. **Tobie J. Matemb Ma Ntep:** Writing - review & editing. **Evangeline Njanja:** Conceptualization, Supervision, Funding acquisition. **Sherman Lesly Zambou Jiokeng:** Validation, Writing - original draft. **Jun Liang:** Investigation, Writing - review & editing. **Christoph Janiak:** Resources, Writing - review & editing. **Ignas Kenfack Tonle:** Conceptualization, Writing - review & editing, Supervision, Funding acquisition.

#### Declaration of Competing Interest

The authors declare that they have no known competing financial interests or personal relationships that could have appeared to influence the work reported in this paper.

#### Acknowledgements

This work was financially supported by the Alexander von Humboldt Foundation (Germany). The German Academic Exchange Service (DAAD) is thanked for a travel grant (no. 57214225) offered to TJMMN.

#### Appendix A. Supplementary data

Supplementary data to this article can be found online at <https://doi.org/10.1016/j.microc.2021.106569>.

#### References

- [1] A.R. Garcia-Fuentes, S. Wirtz, E. Vos, H. Verhagen, Short review of sulfites as food additives, *European J. Nutr. Food Saf.* 5 (2) (2015) 113–120, <https://doi.org/10.9734/EJNFS/2015/11557>.
- [2] I.R.A. Simon, Update on sulfite sensitivity, *Allergy* 53 (46) (1998) 78–79, <https://doi.org/10.1111/j.1398-9995.1998.tb04968.x>.
- [3] H. Vally, N. de Klerk, P.J. Thompson, Alcoholic drinks: important triggers for asthma, *J. Allergy Clin. Immunol.* 105 (3) (2000) 462–467, <https://doi.org/10.1067/mai.2000.104548>.
- [4] L.F. Guido, Sulfites in beer: reviewing regulation, analysis and role, *Sci. Agric.* 73 (2) (2016) 189–197, <https://doi.org/10.1590/0103-9016-2015-0290>.
- [5] Scientific Committee on Food (1994). Opinion on sulfur dioxide and other sulphiting agents used as food preservatives. European Commission, Brussels, Belgium.
- [6] Food and Drug Administration (1986). Food Labeling: Declaration of sulfiting agents. *Fed. Regist.* 51(131) 25012–25020.
- [7] B.R. Hillery, E.R. Elkins, C.R. Warner, D. Daniels, T. Fazio, Optimized monier-williams method for determination of sulfites in foods: collaborative study, *J. AOAC Int.* 72 (3) (1989) 470–475. PMID: 2745372.
- [8] H. Meng, F. Wu, Z. He, Y. Zeng, Chemiluminescence determination of sulfite in sugar and sulfur dioxide in air using Tris(2,2'-bipyridyl)ruthenium(II)-permanganate system, *Talanta* 48 (3) (1999) 571–577, [https://doi.org/10.1016/S0039-9140\(98\)00277-x](https://doi.org/10.1016/S0039-9140(98)00277-x).
- [9] S.W.C. Chung, B.T.P. Chan, A.C.M. Chan, Determination of free and reversibly-bound sulfite in selected foods by high-performance liquid chromatography with fluorometric detection, *J. AOAC Int.* 91 (2008) 98–102, <https://doi.org/10.1093/jaoac/91.1.98>.
- [10] R.C. Claudia, J.C. Francisco, Application of flow injection analysis for determining sulphite in food and beverages, *Rev. Food Chem.* 112 (2) (2009) 487–493, <https://doi.org/10.1016/j.foodchem.2008.05.085>.
- [11] N. Altunay, R.A. Gürkan, New simple UV-Vis spectrophotometric method for determination of sulfite species in vegetable and dried fruits using a preconcentration process, *Anal. Methods* 8 (2) (2016) 342–352, <https://doi.org/10.1039/C5AY02710A>.
- [12] A. Isaac, C. Livingstone, A.J. Wain, R.G. Compton, J. Davis, Electroanalytical methods for the determination of sulfite in food and beverages, *Trends Anal. Chem.* 25 (6) (2006) 589–598, <https://doi.org/10.1016/j.trac.2006.04.001>.
- [13] I. Švancara, K. Vytrás, J. Barek, J. Zima, Carbon paste electrodes in modern electroanalysis, *Crit. Rev. Anal. Chem.* 31 (4) (2001) 311–345, <https://doi.org/10.1080/20014091076785>.
- [14] S. Tajik, H. Beitollahi, F.G. Nejad, M. Safaei, K. Zhang, Q.V. Le, R.S. Varma, H. W. Jang, M. Shokouhimehr, Developments and applications of nanomaterial-based carbon paste electrodes, *RSC Adv.* 10 (36) (2020) 21561–21581, <https://doi.org/10.1039/D0RA003672B>.
- [15] K.M. AlAqad, R. Suleiman, O.C.S. Al Hamouz, T.A. Saleh, Novel graphene modified carbon-paste electrode for promazine detection by square wave voltammetry, *J. Mol. Liq.* 252 (2018) 75–82, <https://doi.org/10.1016/j.molliq.2017.12.108>.
- [16] D. Afzali, S. Zarei, F. Fathirad, A. Mostafavi, Gold nanoparticles modified carbon paste electrode for differential pulse voltammetric determination of eugenol, *Mater. Sci. Eng. C* 43 (2014) 97–101, <https://doi.org/10.1016/j.msec.2014.06.035>.

- [17] J. Wang, A. Walcarius, Zeolite-modified carbon paste electrode for selective monitoring of dopamine, *J. Electroanal. Chem.* 407 (1–2) (1996) 183–187, [https://doi.org/10.1016/0022-0728\(95\)04488-4](https://doi.org/10.1016/0022-0728(95)04488-4).
- [18] L. Liu, Y. Zhou, S. Liu, M. Xu, The application of metal-organic frameworks in electrochemical sensors, *ChemElectroChem* 5 (1) (2018) 6–19, <https://doi.org/10.1039/C8NJ00275E>.
- [19] A.D. Pournara, G.D. Tarlas, G.S. Papaefstathiou, M.J. Manos, Chemically modified electrodes with MOFs for the determination of inorganic and organic analytes via voltammetric techniques, *Crit. Rev. Inorg. Chem. Front.* 6 (12) (2019) 3440–3455, <https://doi.org/10.1039/C9QI00965E>.
- [20] X. Liao, H. Fu, T. Yan, J. Lei, Electroactive metal-organic framework composites: design and biosensing application, *Biosens. Bioelectron.* 146 (2019) 111743, <https://doi.org/10.1016/j.bios.2019.111743>.
- [21] C. Janiak, J.K. Vieth, MOFs, MILs and more: concepts, properties and applications for porous coordination networks (PCNs), *New J. Chem.* 34 (11) (2010) 2366–2388, <https://doi.org/10.1039/C9NJ00275E>.
- [22] D.M. Fernandes, N. Silva, C. Pereira, C. Moura, J.M.C.S. Magalhães, B. Bachiller-Baeza, I. Rodríguez-Ramos, A. Guerrero-Ruiz, C. Delerue-Matos, C. Freire, MnFe<sub>2</sub>O<sub>4</sub>@CNT-N as novel electrochemical nanosensor for determination of caffeine, acetaminophen and ascorbic acid, *Sens. Actuat. B Chem.* 218 (2015) 128–136, <https://doi.org/10.1016/j.snb.2015.05.003>.
- [23] J. Tashkhourian, H. Valizadeh, A. Abbaspour, Ascorbic acid determination based on electrocatalytic behavior of metal-organic framework MIL-101-(Cr) at modified carbon-paste electrode, *J. Assoc. Off. Anal. Chem* 102 (2) (2019) 625–632, <https://doi.org/10.5740/jaoacint.18-0135>.
- [24] G. Férey, C. Mellot-Draznieks, C. Serre, F. Millange, J. Dutour, S. Surblé, I. Margiolaki, A chromium terephthalate-based solid with unusually large pore volumes and surface area, *Science* 309 (5743) (2005) 2040–2042, <https://doi.org/10.1126/science.1116275>.
- [25] D.-Y. Hong, Y.K. Hwang, C. Serre, G. Férey, J.-S. Chang, Porous chromium terephthalate MIL-101 with coordinatively unsaturated sites: surface functionalization, encapsulation, sorption and catalysis, *Adv. Funct. Mater.* 19 (10) (2009) 1537–1552, <https://doi.org/10.1002/adfm.v19:1010.1002/adfm.200801130>.
- [26] Ü. Kökçam-Demir, A. Goldman, L. Esrafilı, M. Gharib, A. Morsali, O. Weingart, C. Janiak, Coordinatively unsaturated metal sites (open metal sites) in metal-organic frameworks: design and applications, *Chem. Soc. Rev.* 49 (9) (2020) 2751–2798, <https://doi.org/10.1039/c9cs00609e>.
- [27] D.M. Fernandes, A.D.S. Barbosa, J. Pires, S.S. Balula, L. Cunha-Silva, C. Freire, Novel composite material polyoxovanadate@MIL-101(Cr): a highly efficient electrocatalyst for ascorbic acid oxidation, *ACS Appl. Mater. Interfaces* 5 (24) (2013) 13382–13390, <https://doi.org/10.1021/am4042564>.
- [28] E.R. Sartori, O. Fatibello-Filho, Simultaneous voltammetric determination of ascorbic acid and sulfite in beverages employing a glassy carbon electrode modified with carbon nanotubes within a Poly(Allylamine Hydrochloride) film, *Electroanalysis* 24 (3) (2012) 627–634, <https://doi.org/10.1002/elan.201100691>.
- [29] Y. Wu, P. Deng, Y. Tian, J. Feng, J. Xiao, J. Li, J. Liu, G. Li, Q. He, Simultaneous and sensitive determination of ascorbic acid, dopamine and uric acid via an electrochemical sensor based on PVP-graphene composite, *J. Nanobiotechnol.* 18 (2020) 112, <https://doi.org/10.1186/s12951-020-00672-9>.
- [30] T. Zhao, F. Jeremias, I. Boldog B. Nguyen, S.K. Henninger, C. Janiak, High-yield fluoride-free and large-scale synthesis of MIL-101(Cr), *Dalton Trans.* 44 (38) (2015) 16791–16801, <https://doi.org/10.1039/C5DT02625C>.
- [31] S. Kayal, B. Sun, A. Chakraborty, Study of metal-organic framework MIL-101(Cr) for natural gas (methane) storage and compare with other MOFs (metal-organic frameworks), *Energy* 91 (2015) 772–781, <https://doi.org/10.1016/j.energy.2015.08.096>.
- [32] N. Li, Q. Zhu, Y. Yang, J. Huang, X. Dang, H. Chen, A novel dispersive solid-phase extraction method using metal-organic framework MIL-101 as the adsorbent for the analysis of benzophenones in toner, *Talanta* 132 (2015) 713–718, <https://doi.org/10.1016/j.talanta.2014.10.038>.
- [33] J. Shadmeh, S. Zeinali, M. Tohidi, Synthesis of a chromium terephthalate metal organic framework and use as nanoporous adsorbent for removal of diazinon organophosphorus insecticide from aqueous media, *J. Dispers. Sci. Technol.* 40 (10) (2019) 1423–1440, <https://doi.org/10.1080/01932691.2018.1516149>.
- [34] Q. Liu, L. Ning, S. Zheng, M. Tao, Y. Shi, Y. He, Adsorption of carbon dioxide by mil-101(cr): regeneration conditions and influence of flue gas contaminants, *Sci. Rep.* 3 (2013) 2916, <https://doi.org/10.1038/srep02916>.
- [35] Y. Shih, J.M. Zen, A.S. Kumar, P. Chen, Flow injection analysis of zinc pyrithione in hair care products on a cobalt phthalocyanine modified screen-printed carbon electrode, *Talanta* 62 (5) (2004) 912–917, <https://doi.org/10.1016/j.talanta.2003.10.039>.
- [36] E. Laviron, General expression of the linear potential sweep voltammogram in the case of diffusionless electrochemical systems, *J. Electroanal. Chem. Interf. Electrochem.* 101 (1) (1979) 19–28, [https://doi.org/10.1016/S0022-0728\(79\)80075-3](https://doi.org/10.1016/S0022-0728(79)80075-3).
- [37] S. Afshaneh, M. Norouz, M. Safieh, T. Fariba, Highly improved electrocatalytic behavior of sulfite at carbon ionic liquid electrode: application to the analysis of some real samples, *Anal. Chim. Acta* 625 (1) (2008) 8–12, <https://doi.org/10.1016/j.aca.2008.07.007>.
- [38] J.A. O'Brien, J.T. Hinkley, S.W. Donne, S.E. Lindquist, The electrochemical oxidation of aqueous sulfur dioxide: a critical review of work with respect to the hybrid sulfur cycle, *Electrochim. Acta* 55 (3) (2010) 573–591, <https://doi.org/10.1016/j.electacta.2009.09.067>.
- [39] S. Lubomir, T. Peter, S. Jana, R. Miroslav, B. Dusan, Determination of caffeine at a nafion-covered glassy carbon electrode, *Food Chem.* 19 (2–3) (2012) 385–388, <https://doi.org/10.1002/elan.200603679>.
- [40] T.R.L. Dadamos, M.F.S. Teixeira, Electrochemical sensor for sulfite determination based on a nanostructured copper-salen film modified electrode, *Electrochim. Acta* 54 (19) (2009) 4552–4558, <https://doi.org/10.1016/j.electacta.2009.03.045>.
- [41] E.M. Silva, R.M. Takeuchi, A.L. Santos, Carbon nanotubes for voltammetric determination of sulphite in some beverages, *Food Chem.* 173 (2014) 763–769, <https://doi.org/10.1016/j.foodchem.2014.10.106>.
- [42] X. Lei, G. Feng, Y. You, J. Hu, Y. Miao, Z. Wu, L. Wang, Simple electrochemical sensor based on carbon-black paste electrode coupled with derivative square wave voltammetry for the determination of sulfites in rice wine, *Int. J. Electrochem. Sci.* 11 (1) (2016) 4586–4597, <https://doi.org/10.20964/2016.06.43>.
- [43] B. Norouzi, Z. Parsa, Zahra, Parsa, Determination of sulfite in real sample by an electrochemical sensor based on Ni/Poly(4-Aminobenzoic Acid)/Sodium Dodecylsulfate/carbon paste electrode, *Russ. J. Electrochem.* 54 (8) (2018) 613–622, <https://doi.org/10.1134/S1023193518080049>.
- [44] P. Kalimuthu, J. Tkac, U. Kappler, J.J. Davis, P.V. Bernhardt, Highly sensitive and stable electrochemical sulfite biosensor incorporating a bacterial sulfite dehydrogenase, *Anal. Chem.* 82 (17) (2010) 7374–7379, <https://doi.org/10.1021/ac101493y>.